Novel Use of Polymer Brushes in Colloidal Lithography To Overcome Lateral Capillary Force

Jun Qian,[†,‡,§] Sarang P. Bhawalkar,[†,§] Yongshen Xu,[‡] and Li Jia*[,†]

Department of Polymer Science, University of Akron, Akron, Ohio 44325-3909, United States, and School of Chemical Engineering and Technology, Tianjin University, Tianjin 300072, China

ABSTRACT A general method has been developed for transferring interfacially trapped, submonolayer hexagonal arrays of silica particles for nano- and mesoscopic surface patterning. Poly(*n*-butyl acrylate) and poly(*n*-butyl acrylate-*random*-*N*,*N*-diethylaminoethyl acrylate) brushes were grafted on the substrates via the "graft-from" method using atom transfer radical polymerization. The polymer brush served as an adhesive promoter between the particles and the substrate and proved to be effective for locking the particles in the hexagonal lattice against the lateral capillary force arising from a thin layer of water attached to the surface of the substrate. Several parameters that influence preservation of the order of the particle arrays were examined. These include brush thickness, brush composition, interparticle distance, and particle diameter.

KEYWORDS: Colloidal lithography • polymer brush • adhesion

INTRODUCTION

Lithographic methods utilizing patterns formed by self-assembled colloidal particles, namely, colloidal lithography (1), have been extensively investigated because they are cost-effective compared to conventional photolithography especially when it comes to patterning large areas despite their limitation of being able to form only simple patterns and highly symmetric patterns. For most practical purposes for patterned surfaces, the individual surface features in a pattern must be separated from each other by a finite distance. For colloidal lithography, this has been achieved by utilizing the interstices of hexagonal close-packed (HCP) colloidal spheres (2), by trimming HCP arrays by shrinking (3) or etching (4), and by shear-induced ordering during spin coating (5−8).

Hexagonal noncontiguously packed (HNCP) crystals of interfacially trapped, like-charged colloidal particles have been a subject of study over the past three decades (9−18). Formation of the two-dimensional crystal is primarily a consequence of minimization of the repulsive electrostatic potential of the like-charged particles confined in a finite area. We have recently explored the use of the HNCP colloidal crystals for surface patterning on the microscopic and nanoscopic length scales (19, 20). The process is conceptually simple. Transfer of the colloidal crystals from the air−water interface can be accomplished by generating electrostatic and van der Waals attractions between the particles and the solid substrate. The electrostatic and van der Waals attractions are also expected to overcome lateral capillary force acting on the particles when a thin film of water inevitably brought onto the solid substrate in the transfer process dries.

Scheme 1. Strategies for Immobilizing Particles on Substrates

It turned out that preservation of the pattern against the lateral capillary force in the drying stage after the initial transfer is the challenging part of the patterning process. Adhesion between a hard sphere and a hard surface is usually too weak to withstand the lateral capillary force (21). We have resorted to a few tactics to deal with this problem. First, a fluid-exchange process was implemented to displace the water thin film with an organic fluid, e.g., ethanol (19). Because the magnitude of the lateral capillary force is proportional to surface tension, switching from water to ethanol results in a more than 3-fold reduction in the lateral capillary force under otherwise identical situations. This tactic allows for retention of only the HNCP patterns with a relatively large interparticle distance (see discussion below for the effect of interparticle distance on the magnitude of lateral capillary force). A more secure method involves inclusion of a solvent in the organic fluid to swell the latex particles and consequently create a large area of contact between the particles and the solid substrate as illustrated in Scheme 1. Use of latex particles with a soft shell also provides a way to generate a relatively large contact area between the particles and the substrate (20). However, the latex particles with a soft shell flocculate in alcohols, which are commonly used for spreading the particles onto the

* To whom correspondence should be addressed.
Received for review July 12, 2010 and accepted October 8, 2010
† University of Akron.
‡ Tianjin University.
§ J.Q. and S.P.B. contributed equally to the work.
DOI: 10.1021/am100608k

air−water interface. As a result, interfacial trapping of the soft shell particles was realized by agitation, which is inferior to spreading as it does not yield a predictable number of particles per unit area at the interface. In any case, the tactics that rely on particle deformation cannot be applied to particles that are not easily deformed. Such a limitation is a major detriment because inorganic particles, which impart a variety of useful properties such as magnetism, quantum effects, plasma etch resistance, etc., are obviously hard and not readily deformable.

To meet the need for a general method that can be applied to inorganic particles, we explored an alternative venue for improving adhesion between the particles and the substrate. Polymer brushes are versatile and effective for tuning surface properties such as wetting and adhesion (22−27) but have not been used in the context of surface patterning. The method reported here involves functionalization of the substrate with a polymer brush using a "graft-from" method (28, 29). The polymer has a low glass transition temperature in bulk and is expected to serve as an adhesive that immobilizes the particles (Scheme 1). Parameters that influence the effectiveness of the polymer brush in retaining the pattern are investigated, including the thickness and composition of the polymer brush, particle size, and interparticle distance.

EXPERIMENTAL SECTION

Materials. Monodisperse silica particles with average diameters of 100, 250, 500, and 750 nm (standard deviation of <10%) were purchased from Angströmsphere. 2-(*p-tert*-Butylphenyl)ethyltrichlorosilane (BPTCS, Gelest) and 2-(4-chlorosulfonylphenyl)ethyltrichlorosilane (SPTCS, Gelest) were used as received. *n*-Butyl acrylate (n-BA, >99%, Aldrich) was purified when it was passed through a basic alumina column before use. *N*,*N*-Diethylaminoethyl acrylate (DEAEA, 95%, Aldrich) was purified by vacuum distillation. Copper(I) bromide (98%, Aldrich) was purified according to the literature (30). Ethyl 2-bromoisobutyrate (E_2Br-iB, 98%, Aldrich) and *N*,*N*,*N*′,*N*′,*N*″-pentamethyldiethylenetriamine (PMDETA, 99%, Aldrich) were used as received. 11-(2-Bromo-2-methyl)propionyloxyundecyltrichlorosilane (BMPUS) was synthesized according to a literature method (15). Anisole (99.7%, anhydrous, Aldrich), toluene (99.8%, anhydrous, Aldrich), ethanol (anhydrous, Aldrich), and triethylamine (99%, Aldrich) were used as received. Silicon wafers were purchased from Wafer World.

Ellipsometry Measurements. Ellipsometry measurements were taken on a Gaertner model L116C ellipsometer with a He−Ne laser ($\lambda = 632.8$ nm) and a fixed angle of incidence of 70°. For the thickness calculations, the following refractive indices were used: $n = 1.455$ for the native silicon oxide, $n = 1.508$ for the initiator monolayer, and $n = 1.466$ for the polymer layer (31).

Contact Angle Measurements. Water contact angles were measured via the sessile drop technique on a Rame-Hart (Mountain Lake, NJ) goniometer (model 100-00) using deionized water under ambient conditions. The drop size used was 10 μL. Three spots on each substrate were chosen for static contact angles. The average was calculated from two independent samples and reported as the mean ± the standard deviation.

Molecular Weight Determination. The molecular weights of the free polymers in solution were determined by gel permeation chromatography (GPC) using three Waters HR styragel columns in tetrahydrofuran at 35 °C at a flow rate of 1 mL/min. A Wyatt DAWN EOS multiangle laser light scattering (MALLS) detector with a Waters model 410 differential refractometer concentration detector was used.

Atomic Force Microscopy (AFM) Studies. The surface topology and roughness of the silicon substrates modified with the polymer brushes were characterized by AFM in the tapping mode. Briefly, samples were rinsed with THF and dried with filtered air. A Multimode NanoScope IIId AFM System (Veeco Inc.) operated in air and commercial silicon nitride cantilevers (DI) with an elastic modulus of 0.56 N/m were used. The surface roughness was calculated using the imaging software Solver P47 according to the following definition:

$$R_q = \sqrt{\frac{1}{N}\sum_{i=1}^{N}(z_i - z_{av})^2}$$

where R_q is the root-mean-square roughness, z_i is the height value for a specific pixel, z_{av} is the average of the z_i values, and N is the number of pixels in the scanned area.

Electron Microscopy and Method of Image Analysis. The particle patterns were imaged via scanning electron microscopy (SEM, JEOL-6300f). All SEM samples were sputter-coated with Au (Polaron E5100 SEM coating unit) to make the surface conductive. Fourier transformation of the SEM micrographs was performed using Fourier Transform Lab-Student Edition (FTL-SE).

Functionalization of Silica Particles. Silica particles (0.32 g) were dried in a vacuum oven for 24 h at 100 °C prior to functionalization. The particles were dispersed in anhydrous ethanol (50 mL) in a Schlenk flask and sonicated with a Fisher Scientific sonicator for 2 h. BPTCS (0.70 mL, 2.75 mmol) and SPTCS (0.30 mL, 0.61 mmol) were added to the mixture while the particles were being sonicated. After 1 h, triethylamine (1.5 mL, 10.4 mmol) was added to the flask, and the reaction was allowed to continue for 20 h at room temperature. After the reaction was completed, the particles were washed with ethanol via four centrifugation−redispersion cycles to remove the excess silanes. The particles were then dried and stored for further use.

Synthesis of Polymer Brushes. Silicon wafers were cut into approximately 1.8 cm × 4.2 cm rectangles so that they fit into the reaction flasks for surface functionalization. They were first functionalized by the ATRP initiator BMPUS following the literature procedure (15). The procedure for the synthesis of the polymer brush from the same work in the literature was used after minor modifications. All operations were conducted under nitrogen protection. Typically, a solution containing PMDETA, anisole, and the monomer was added to a Schlenk flask and subjected to three freeze−pump−thaw cycles. Then the solution was cannulated into another Schlenk flask containing CuBr. The mixture was stirred at 90 °C and became homogeneous in ~10 min. At this time, the homogeneous solution was cannulated into a third Schlenk flask that held the BMPUS-functionalized silicon wafers to start the ATRP from the surface. The solution phase initiator E_2Br-iB was added immediately to the reaction mixture with a syringe. The polymerization proceeded at 90 °C for 2 days. After the reaction, the substrate was removed and washed sequentially with dichloromethane, tetrahydrofuran, and 2-propanol. To remove any free polymer chains, we placed the substrate in a Soxhlet extractor and extracted the substrate with tetrahydrofuran for 24 h followed by sonication in tetrahydrofuran for 30 min. The substrate was then dried with a nitrogen jet and kept for use. The polymer produced in the solution phase was used for molecular weight measurement.

Interfacial Particle Film Formation and Transfer. The particle film at the air−water interface was formed in a Nima Langmuir−Blodgett trough (model 102M-A). The trough had two mechanically movable barriers, which allow the interfacial area

Scheme 2. HNCP Spheres Inscribed by Hexagons

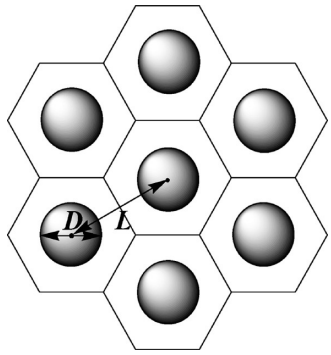

to be adjusted from 80.5 to 11.5 cm^2. Typically, a 1−3 wt % dispersion of the functionalized particles in 2-propanol (20−60 μL) was spread onto the surface of deionized water at a rate of 60 μL/h using a 100 μL Hamilton syringe and a KD Scientific syringe pump (model 780100). After the particles were allowed to equilibrate for a few minutes at room temperature, the barriers were compressed to achieve a desired area of confinement at a speed of 5 cm^2/min. To improve the regularity of the particle arrays, we conducted compression−expansion cycles. The expansion was performed at the same speed (5 cm^2/min) as the compression. Transfer of the interface particle arrays was conducted using the Langmuir−Schaefer technique in which the substrate was lowered horizontally toward the interface and brought into contact with the interface. This should result in complete transfer of the particles to the substrate. The residual water on the substrate was blown dry with a nitrogen jet.

Variation of Interparticle Distance. A known weight amount (M) of the particles was spread onto the air−water interface as described above. The mass of each individual particle, m, can be calculated by the formula $m = \rho V = \rho(4\pi)/(3)(D/2)^3$, where ρ is the density of the particle and is specified by the supplier to be 1.8 g/cm^3, V is the particle volume, and D is the particle diameter. The total number of particles at the interface, Z, therefore becomes known from the relationship $Z = M/m$. In an HNCP lattice, each sphere can be inscribed by a concentric hexagon as illustrated in Scheme 2. The area of each hexagon is $(3/2)^{1/2}L^2$, so $Z(3/2)^{1/2}L^2$ is the total area occupied by the hexagons. This area is equal to the experimentally adjustable area between the movable barriers of the trough, A. Therefore, the interparticle distance, L, can be controlled according to the relationship $L = (2A)^{1/2}/(3Z)^{1/2}$.

RESULTS AND DISCUSSION

Functionalization of the Substrate. The surface of the substrate performs two functions in transferring the interfacial HNCP pattern formed by the charged particles at the air−water interface. First, it effects complete adsorption of the particles onto the substrate when the substrate is brought into contact with the particles. This is usually not a problem as long as the surface of the substrate is not easily wetted by water or, in our hands, has an advancing contact angle of >70° to be safe. Second, it keeps the order of the particles intact after the particles are adsorbed on the substrate. This is the difficult part of the transfer process and requires strong adhesion between the particles and the substrate. Hydrophobic polymer adhesives are natural choices for performing the functions described above. We opt in this work to use the polymer brush strategy so that the thickness and composition of the adhesive layer can be adjusted and the layer is not easily detached from the substrate.

ATRP initiated by surface-bound BMPUS was adopted to synthesize the polymer brush (15). n-BA was used as the base monomer that provides the low glass transition temperature (T_g) essential for a room-temperature adhesive. DEAEA was used as a minor comonomer to introduce charge as the amino units are protonated at neutral pH. Synthesis of the polymer brush and the properties of the resulting brush-covered surfaces are summarized in Table 1.

The thickness of the polymer brush was controlled by the concentration of the monomers. The molecular weight of the polymer brush was estimated by analyzing the free polymer in solution simultaneously produced by the "free" initiator E_2Br-iB as it has been shown that the molecular weight of the free polymer is comparable to that of the polymer brush (32, 33). The trend in the brush thickness was consistent with the trend in the molecular weight. The ratio of the incorporated comonomers in the free copolymer was the same as the feed ratio (80:20 n-BA:DEAEA molar ratio) according to ^{1}H NMR analysis. By inference, the composition of the copolymer brush was likely similar to the feed ratio, too. The contact angles of all four brush-covered substrates were adequately high for the purpose of particle adsorption.

The surface topographies of randomly chosen areas of substrates **homo-31** and **co-12** were investigated by AFM (Figure 1). The root-mean-square roughness (R_q) was only a few percent of the brush thickness measured by ellipsometry in both cases (Table 1). The low surface roughness on the

Table 1. Synthesis and Characterization of Polymer Brushes[a]

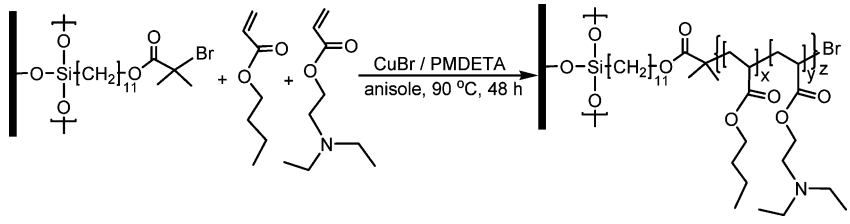

substrate	n-BA (mmol)	DEAEA (mmol)	M_n[b] ($\times 10^3$ g/mol)	PDI[b]	brush thickness[c] (nm)	R_q (nm)	contact angle (deg)
homo-12	70.0	−	15	1.15	12.0 ± 2.0		87 ± 3
homo-31	139.5	−	31	1.21	31.0 ± 2.7	0.877	88 ± 2
co-5	42.0	10.5	11	1.30	5.0 ± 1.1		78 ± 1
co-12	78.0	19.5	18	1.26	12.0 ± 2.6	0.414	80 ± 2

[a] For 0.39 mmol of CuBr and 0.75 mmol of PMDETA. Free initiator was present in all cases, yielding free polymer simultaneously (0.31 mmol of E_2Br-iB). [b] Determined by GPC. [c] Determined by ellipsometry.

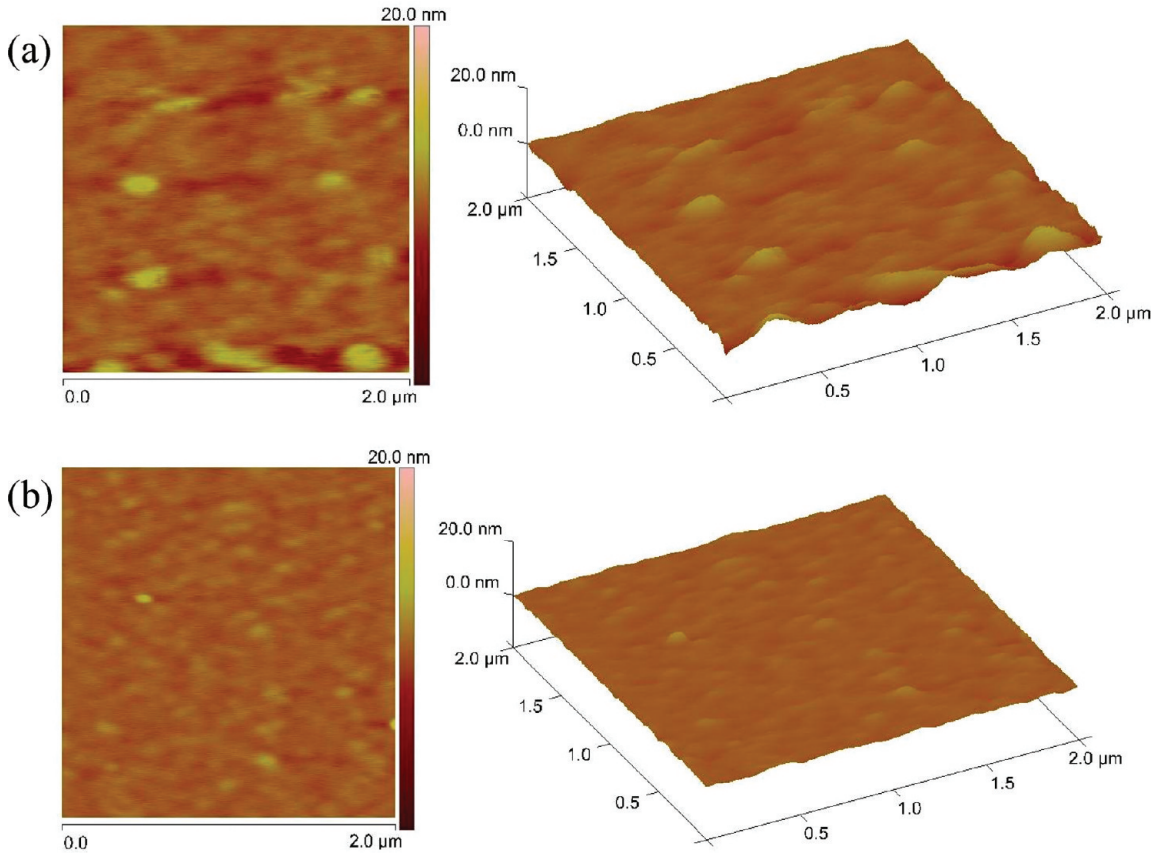

FIGURE 1. AFM topographic images of polymer brush-functionalized substrates: (a) substrate homo-31 and (b) substrate co-12.

microscopic scale and the small variation in the thickness values on the macroscopic scale confirm uniform coverage of the polymer brush on the substrate. The uniformity of the polymer brush is essential because a small defective area may trigger a cascade of imbalance of the lateral capillary force and result in the destruction of a disproportionately large fraction of the HNCP particle arrays.

Pattern Formation and Pattern Transfer. For the particles to be trapped at the air−water interface and to self-assemble into the HNCP lattice, the surface of the particles must have a sufficiently high water contact angle (34) and be sufficiently charged (9). Treatment of the silica particles with a mixture of BPTCS and SPTCS in a 70:30 volume ratio (82:18 molar ratio), empirically adopted as it gave a static contact angle of 72 ± 3° on a flat glass surface, proved to be satisfactory for the interfacial trapping and self-assembly. To form the interfacial particle film, we dispersed the surface-modified silica particles in 2-propanol and spread them onto the air−water interface in a Langmuir trough. The particle film was compressed with the movable barriers of the trough to bring the particles within the range of the electrostatic repulsion for self-assembly. The modified silicon substrate was horizontally brought into contact with the water surface and withdrawn. The substrate was then dried with a nitrogen flow.

The macroscopic appearance of the wafer can usually provide the first indication about whether the order of the particle array is retained on the substrate (Figure 2). Even a

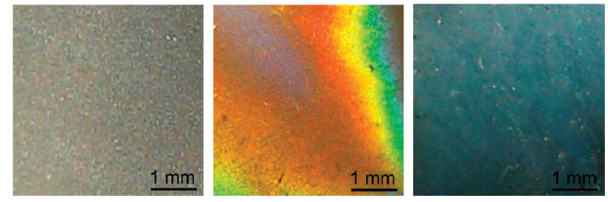

FIGURE 2. Macroscopic appearance of wafers with (left) disordered 250 nm silica particles, (center) HNCP 250 nm silica particles, and (right) HNCP 100 nm silica particles.

multigrained HNCP array such as the one in Figure 3a is usually sufficient to generate the angle-dependent iridescent colors, with the exception of the 100 nm particles. The HNCP 100 nm particles brought a dull blue color blended with vague luster to the substrate, indicating that scattering overtakes diffraction in color display. An increase in the relative intensity of the non-zeroth-order diffractions and the insufficient long-range order of the pattern are likely both responsible for the change in the color display mode. The long-range order of the particles can be improved by subjecting the interfacial film to compression−expansion cycles. This is clearly evident from the Fourier transformed (FT) images (Figure 3). The periodicities corresponding to the (10), (01), and (11) crystal lines were barely observable with one compression. After five compression−expansion cycles, the periodicities corresponding to the (12), (21), and $(1\bar{1})$ crystal lines appeared. After 15 cycles, the periodicities corresponding to the (13), (32), $(2\bar{1})$, (31), (23), and $(\bar{1}2)$

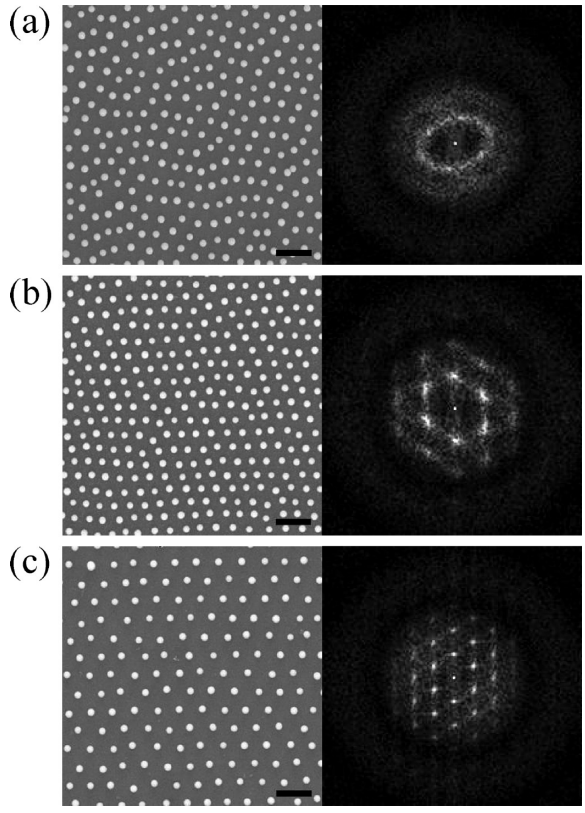

FIGURE 3. SEM and FT images of 250 nm particles on substrate co-12 after one compression (a), after five compression−expansion cycles (b), and after 15 compression−expansion cycles (c). The scale bar is 1 μm.

crystal lines appeared. In this work, we routinely performed 15 compression−expansion cycles for each experiment.

Both the thickness and the chemical composition of the polymer brush are critical for the preservation of the particle pattern on the substrate. The patterns formed by the 100, 250, and 370 nm particles (see below for a discussion of larger particles) were usually intact on substrates **homo-31** and **co-12** but were destroyed on substrates **homo-12** and **co-5**. The two pairs of substrates, **homo-31** versus **homo-12** and **co-12** versus **co-5**, bear the brushes with the same comonomer compositions but differ in brush thickness. Therefore, a minimum brush thickness is necessary to generate adequate adhesion to lock the particles in place. This can likely be attributed to a larger contact area generated by a thicker brush and therefore a greater total work of adhesion between the particles and the substrate. AFM measurements revealed that the particles were indeed partially buried in the brush. For example, the 250 nm particles were 229.9 ± 13.8 nm (64 measurements) high on substrate **homo-31** in comparison to 249.4 ± 9.0 nm (30 measurements) on a bare silicon wafer. Because the brush thicknesses on substrates **homo-12** and **co-12** are approximately same, the difference in their ability to retain the particle order can be attributed to the electrostatic attraction between the positively charged brush (i.e., **co-12**) and the negatively charged particles.

Grafting density is obviously another critical parameter that affects the interaction between the brushes and particles (35). It appears, fortunately, that the presently adopted method gives the appropriate grafting density for the polymer brushes to work as adhesive promoters. Two sets of systematic experiments were subsequently conducted to further evaluate the ability of substrates **homo-31** and **co-12** to lock the particles in the lattice.

Patterns with Varied Interparticle Distances. The magnitude of the lateral capillary force is strongly dependent on the interparticle distance. A comprehensive theoretical treatment of the lateral capillary force between two colloidal particles partially immersed in a water film has been given by Kralchevsky et al. (36, 37). The numerical solutions to the complex analytical expression show that the lateral capillary force increases sharply as the interparticle distance (L, i.e., the center-to-center distance of two particles) is reduced, especially when the magnitude of L is comparable to the particle diameter (D). In a separate study, they also demonstrated using glass spheres 600 μm in diameter that the theoretical predictions were consistent with the experimentally measured values (38).

We investigated the transfer of a series of HNCP particles with varied L to probe the limit of the minimum L achievable using substrates **homo-31** and **co-12**. The particles with a diameter of 250 nm (i.e., $D = 250$ nm) were arbitrarily chosen for the series of experiments. Figure 4 shows the SEM images of the transferred particles on the substrates. Well-order HNCP patterns do not form at the air−water interface when $L \geq 3D$ apparently because of inadequate electrostatic repulsion but do form when $L \leq 2.5D$. Both substrates are able to retain the HNCP patterns when $2.5D \geq L \geq 1.5D$. When $L = 1.2D$, substrate **homo-31** is unable to retain the pattern but **co-12** is able to. Neither is able to retain the pattern when $L = 1.1D$. When $L = 1.0D$, the particles are close-packed. The experiments confirm that the HNCP patterns with a very narrow interparticle separation pose a challenge for the present surface patterning method. Thick polymer brushes would be necessary to push the limit.

Effects of Particle Size on Pattern Preservation. While the magnitude of the lateral capillary force is the single important variable that changes upon variation of the interparticle distance, a change in the particle diameter causes changes in both the adhesion forces and the lateral capillary force. The theoretical work of Kralchevsky et al. (36, 37) predicted a significant increase in the lateral capillary force between two particles at a fixed interparticle distance when the particle diameter increased. Practically, however, when the particles with a different diameter are used to form the HNCP crystal, the achievable interparticle distance scales with the diameter. As discussed above, the increase in the interparticle distance would contribute to weakening the capillary force, which is opposite to the effect of a particle diameter increase. From the perspective of adhesion strength, the increase in particle diameter would result in an increase in the contact area between the polymer brush and the particles and in turn an increase in the overall adhesion strength. Further, if the particles migrate by rolling instead of sliding, the increase

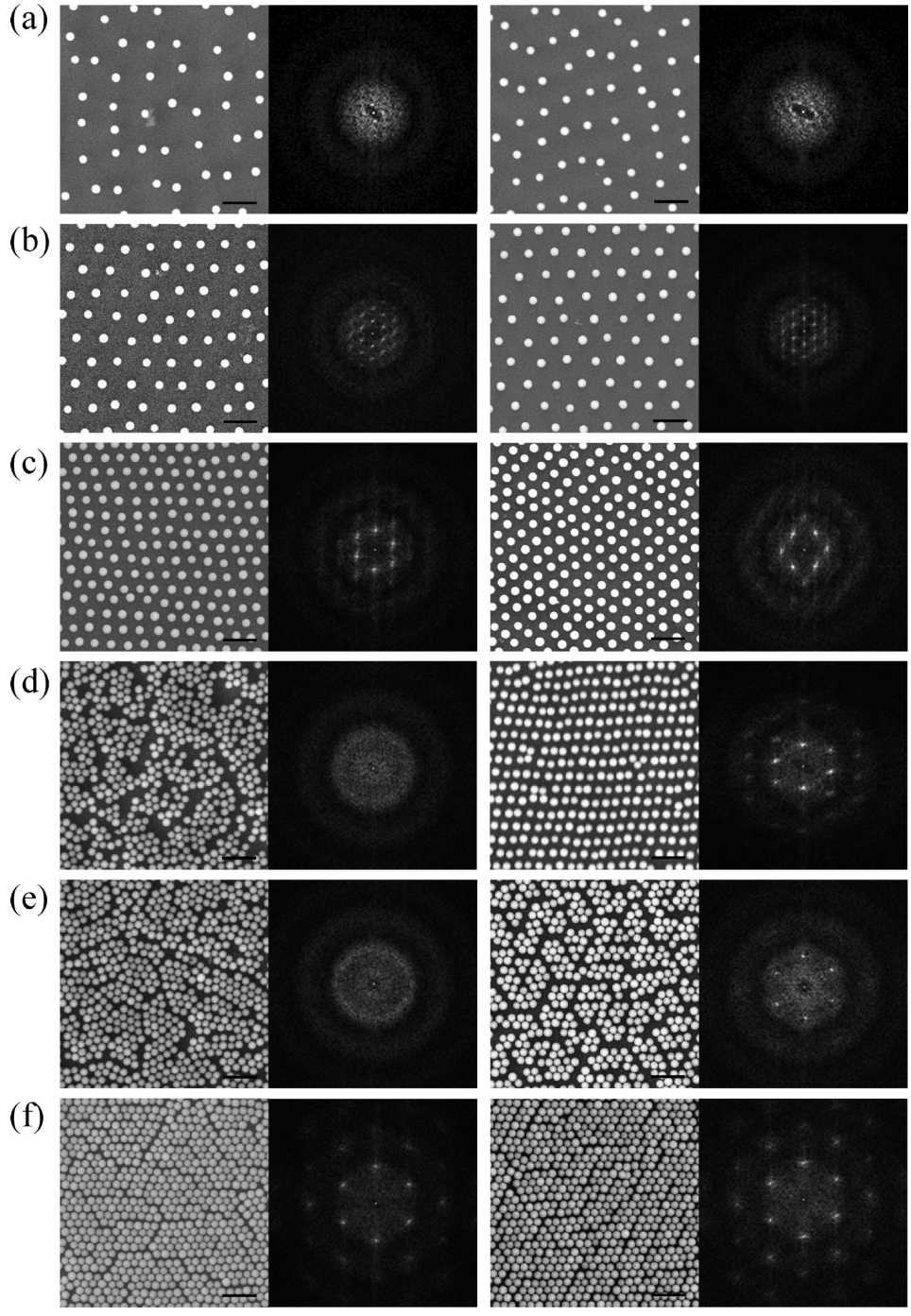

FIGURE 4. SEM and Fourier transform images of 250 nm silica particle arrays with various anticipated *L* values after being transferred onto substrates homo-31 (left) and co-12 (right). (a) $L = 3.0D$. (b) $L = 2.5D$. (c) $L = 1.5D$. (d) $L = 1.2D$. (e) $L = 1.1D$. (f) $L = 1.0D$. The scale bar is 1 μm.

in particle diameter would result in an increase in the torques of moments from both the adhesion force and the capillary force (39).

The very complex scenario upon variation of the particle size prompted us to investigate transfer of the HNCP particles of various sizes. A reasonably large variation of the particle diameter was implemented with monodisperse silica particles 100, 250, 370, 500, and 750 nm in diameter. Substrates **homo-31** and **co-12** were again used. The *L*/*D* ratio in the HNCP patterns was kept constant at 2. Figure 5 shows the SEM images after the particles were transferred from the air−water interface onto the substrates. The patterns remained intact for the 100, 250, and 370 nm particles but were almost completely destroyed for the 750 nm particles. The 500 nm particle represented a borderline case, where the patterns were partially retained particularly when **co-12** was used as the substrate. The experiments described above clearly demonstrate that overall, the HNCP patterns of larger particles are more difficult to preserve than those of smaller particles.

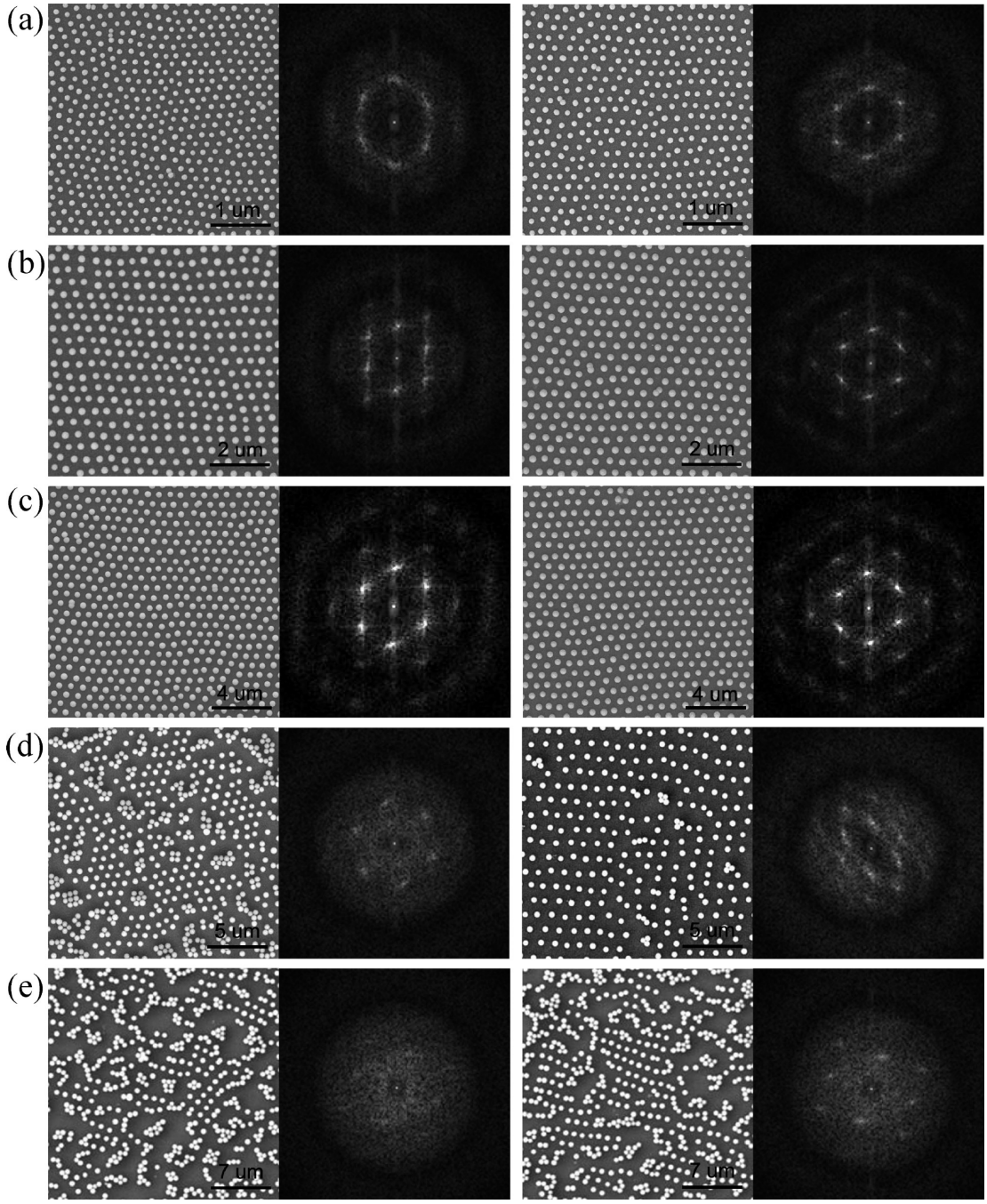

FIGURE 5. SEM images and Fourier transformed images of silica particles with *D* values of 100 (a), 250 (b), 370 (c), 500 (d), and 750 nm (e) after being transferred onto substrates homo-31 (left) and co-12 (right).

CONCLUSION

We have demonstrated that polymer brushes can be used as adhesion promoters in a colloidal lithography process. The process is an important improvement over what we have previously developed because it does not require deformation of the particles and therefore can in principle be applied to all inorganic particles. This provides an opportunity to use electronically, magnetically, and optically functional inorganic particles to pattern solid substrates. A minimum brush thickness is required for immobilizing the particles on the substrate against the destructive lateral capillary force. The chemical composition of the brush is also important for immobilizing the particles. Preservation of the HNCP pattern becomes increasingly challenging as the interparticle distance is reduced or the particle diameter is increased. The effect of particle diameter usually dominates over the effect of the interparticle distance.

Acknowledgment. We thank the University of Akron for financial support of this work (L.J., startup). J.Q. thanks the China Scholarship Council (CSC) for awarding him a scholarship and Tianjin University for giving him the opportunity to pursue his study in the United States as a Joint Ph.D. Student. L.J. thanks the Office of Research Services and Sponsored Programs of the University of Akron for a Faculty Research Grant. We also thank the National Science Foundation (CHE-9977144) for funding the University of Akron

Magnetic Resonance Center's purchase of the nuclear magnetic resonance instrument used in this work.

REFERENCES AND NOTES

(1) Velev, O. D.; Gupta, S. *Adv. Mater.* **2009**, *21*, 1897.
(2) Hulteen, J. C.; Treichel, D. A.; Smith, M. T.; Duval, M. L.; Jensen, T. R.; Van Duyne, R. P. *J. Phys. Chem. B* **1999**, *103*, 3854.
(3) Zhang, G.; Wang, D.; Gu, Z.-Z.; Hartmann, J.; Möhwald, H. *Chem. Mater.* **2005**, *17*, 5268.
(4) Plettl, A.; Enderle, F.; Saitner, M.; Manzke, A.; Pfahler, C.; Wiedemann, S.; Ziemann, P. *Adv. Funct. Mater.* **2009**, *19*, 3279.
(5) Min, W.-L.; Jiang, P.; Jiang, B. *Nanotechnology* **2008**, *19*, 475604/1-7.
(6) Min, W.-L.; Jiang, B.; Jiang, P. *Adv. Mater.* **2008**, *20*, 3914.
(7) Venkatesh, S.; Jiang, P.; Jiang, B. *Langmuir* **2007**, *23*, 8231.
(8) Jiang, P.; McFarland, M. J. *J. Am. Chem. Soc.* **2005**, *127*, 3710.
(9) Pieranski, P. *Phys. Rev. Lett.* **1980**, *45*, 569.
(10) Onoda, G. Y. *Phys. Rev. Lett.* **1985**, *55*, 226.
(11) Armstrong, A. J.; Mockler, R. C.; O'Sullivan, W. J. *J. Phys.: Condens. Matter* **1989**, *1*, 1707.
(12) Robinson, D. J.; Earnshaw, J. C. *Langmuir* **1993**, *9*, 1436.
(13) Ruiz-García, J.; Gámez-Corrales, R.; Ivlev, B. I. *Phys. Rev. E* **1998**, *58*, 660.
(14) Aveyard, R.; Clint, J. H.; Nees, D.; Paunov, V. N. *Langmuir* **2000**, *16*, 1969.
(15) Ghezzi, F.; Earnshaw, J. C.; Finnis, M.; McCluney, M. *J. Colloid Interface Sci.* **2001**, *238*, 433.
(16) Nikolaides, M. G.; Bausch, A. R.; Hsu, M. F.; Dinsmore, A. D.; Brenner, M. P.; Gay, C.; Weitz, D. A. *Nature* **2002**, *420*, 299.
(17) Megens, M.; Aizenberg, J. *Nature* **2003**, *424*, 1014.
(18) Aveyard, R.; Binks, B. P.; Clint, J. H.; Fletcher, P. D. I.; Horozov, T. S.; Neumann, B.; Paunov, V. N. *Phys. Rev. Lett.* **2002**, *88*, 246102.
(19) Ray, M. A.; Jia, L. *Adv. Mater.* **2007**, *19*, 2020.
(20) Ray, M. A.; Shewmon, N.; Bhawalkar, S.; Jia, L.; Yang, Y.; Daniels, E. S. *Langmuir* **2009**, *25*, 7265.
(21) Thill, A.; Spalla, O. *Langmuir* **2002**, *18*, 4783.
(22) Advincula, R., Brittain, W. J., Caster, K., Rühe, J., Eds. *Polymer Brushes*; Wiley-VCH Verlag: Weinheim, Germany, 2004; Chapters 17–23.
(23) (a) Uhlmann, P.; Merlitz, H.; Sommer, J.-U.; Stamm, M. *Macromol. Rapid Commun.* **2009**, *30*, 732.
(24) Rühe, J.; Ballauff, M.; Biesalski, M.; Dziezok, P.; Gröhn, F.; Johannsmann, D.; Houbenov, N.; Hugenberg, N.; Konradi, R.; Minko, S.; Motornov, M.; Netz, R. R.; Manfred Schmidt, M.; Seidel, C.; Stamm, M.; Stephan, T.; Usov, D.; Zhang, H. *Adv. Polym. Sci.* **2004**, 79.
(25) Gupta, S.; Agrawal, M.; Uhlmann, P.; Simon, F.; Oertel, U.; Stamm, M. *Macromolecules* **2008**, *41*, 8152.
(26) Ionov, L.; Sapra, S.; Synytska, A.; Rogach, A. L.; Stamm, M.; Diez, S. *Adv. Mater.* **2006**, *18*, 1453.
(27) Advincula, R., Brittain, W. J., Caster, K., Rühe, J., Eds. *Polymer Brushes*; Wiley-VCH Verlag: Weinheim, Germany, 2004; Chapters 17–23.
(28) Zhao, B.; Brittain, W. J. *Prog. Polym. Sci.* **2000**, *25*, 677.
(29) Matyjaszewski, K.; Miller, P. J.; Shukla, N.; Immaraporn, B.; Gelman, A.; Luokala, B. B.; Siclovan, T. M.; Kickelbick, G.; Vallant, T.; Hoffmann, H.; Pakula, T. *Macromolecules* **1999**, *32*, 8716.
(30) Keller, R. N.; Wycoff, H. D. *Inorg. Synth.* **1947**, *2*, 1.
(31) Brandrup, J. In *Polymer Handbook*; Immergut, E. H., Grulke, E. A., Eds.; Wiley and Sons: New York, 1999; pp III-241–III-243.
(32) Husemann, M.; Malmstrom, E. E.; McNamara, M.; Mate, M.; Merreceyes, D.; Benoit, D. G.; Hedrick, J. L.; Mansky, P.; Huang, E.; Russell, T. P.; Hawker, C. J. *Macromolecules* **1999**, *32*, 1424–1431.
(33) Baum, M.; Brittain, W. J. *Macromolecules* **2002**, *35*, 610.
(34) Binks, B. P. *Curr. Opin. Colloid Interface Sci.* **2002**, *7*, 21.
(35) Brittain, W. J.; Minko, S. *J. Polym. Sci., Part A: Polym. Chem.* **2007**, *45*, 3505.
(36) Kralchevsky, P. A.; Nagayama, K. *Langmuir* **1994**, *10*, 23.
(37) Kralchevsky, P. A.; Paunov, V. N.; Inanov, I. B.; Nagayama, K. *J. Colloid Interface Sci.* **1992**, *151*, 79.
(38) Dushkin, C. D.; Kralchevsky, P. A.; Yoshimura, H.; Nagayama, K. *Phys. Rev. Lett.* **1995**, *75*, 3455.
(39) Sharma, M. M.; Chamoun, H.; Sarma, D. S. H.; Sita, R.; Schechter, R. S. *J. Colloid Interface Sci.* **1992**, *149*, 121.

AM100608K